

Calculation of renormalized viscosity and resistivity in magnetohydrodynamic turbulence

Mahendra K. Verma^{a)}

Department of Physics, Indian Institute of Technology, Kanpur 208016, India

(Received 30 January 2001; accepted 1 May 2001)

A self-consistent renormalization (RG) scheme has been applied to nonhelical magnetohydrodynamic turbulence with normalized cross helicity $\sigma_c=0$ and $\sigma_c \rightarrow 1$. Kolmogorov's $\frac{5}{3}$ power law is assumed in order to compute the renormalized parameters. It has been shown that the RG fixed point is stable for $d \geq d_c \approx 2.2$. The renormalized viscosity ν^* and resistivity η^* have been calculated, and they are found to be positive for all parameter regimes. For $\sigma_c=0$ and large Alfvén ratio (ratio of kinetic and magnetic energies) r_A , $\nu^*=0.36$, and $\eta^*=0.85$. As r_A is decreased, ν^* increases and η^* decreases, until $r_A \approx 0.25$, where both ν^* and η^* are approximately zero. For large d , both ν^* and η^* vary as $d^{-1/2}$. The renormalized parameters for the case $\sigma_c \rightarrow 1$ are also reported.

© 2001 American Institute of Physics. [DOI: 10.1063/1.1389298]

I. INTRODUCTION

The renormalization group (RG) technique provided an important tool for an understanding of the phenomena of phase transitions and critical phenomena. Motivated by this success, researchers have applied this technique to turbulence and other nonequilibrium systems. In this paper we apply RG to magnetohydrodynamic (MHD) turbulence.

Forster *et al.*¹ first applied a dynamical RG procedure to the analysis of Navier–Stokes and Burgers equations, both stirred by random forces. They eliminated the large-wave number modes and included the effects of nonlinearity in the effective viscosity. Later, DeDominicis and Martin,² Fournier and Frisch,³ Yakhot and Orszag,⁴ and many others studied various aspects of RG for fluid turbulence, but all of them considered certain forms of external forcing. McComb and his co-workers (see Refs. 5, 6 and references therein) instead applied a self-consistent RG procedure; here the energy spectrum was assumed to be Kolmogorov's spectrum, and the renormalized viscosity was computed iteratively. We have adopted a similar scheme for MHD turbulence.

Fournier *et al.*,⁷ Camargo and Tasso,⁸ and Liang and Diamond⁹ applied a RG technique to MHD turbulence on lines similar to those adopted by Forster *et al.*¹ for fluid turbulence. Fournier *et al.*⁷ found that for $d > d_c \approx 2.8$, there are two nontrivial regimes: a kinetic regime where the renormalization of the transport coefficients is due to kinetic small scales; and a magnetic regime where it is due to the magnetic small scales. In dimensions $2 \leq d \leq d_c$, there is no stable fixed point for turbulence with sufficiently strong external currents. Camargo and Tasso⁸ studied the effective (renormalized) viscosity and resistivity and concluded that negative viscosity and resistivity are not permissible except in certain cases. Liang and Diamond⁹ showed that no RG fixed point exists in two-dimensional (2-D) MHD turbulence. All the above authors, however, do not give any clear idea about

the energy spectrum of MHD turbulence, which still remains controversial. However, Verma¹⁰ used a technique similar to that of McComb and co-workers (see Refs. 5, 6 and references therein) and showed that Kolmogorov's spectrum is a consistent solution of MHD RG equations.

Kraichnan¹¹ and Iroshnikov¹² first gave the phenomenology of steady-state, homogeneous, and isotropic MHD turbulence. They argued that the kinetic and magnetic energy spectra [$E^u(k)$ and $E^b(k)$, respectively] are

$$E^u(k) = E^b(k) = A(\Pi B_0)^{1/2} k^{-3/2}, \quad (1)$$

where Π is the total energy cascade rate, B_0 is the mean magnetic field or the magnetic field of the largest eddy, and A is a universal constant of order one. Later, Matthaeus and Zhou,¹³ and Zhou and Matthaeus¹⁴ proposed a generalized phenomenology in which the cascade rates Π^\pm and energy spectra $E^\pm(k)$ of Elsässer variables $\mathbf{z}^\pm (= \mathbf{u} \pm \mathbf{b})$ are related by

$$\Pi^\pm = \frac{A^2 E^+(k) E^-(k) k^3}{B_0 + \sqrt{k E^\pm(k)}}, \quad (2)$$

where A is a constant. In the limit $B_0=0$, we can immediately obtain

$$E^\pm(k) = K^\pm \frac{(\Pi^\pm)^{4/3}}{(\Pi^\mp)^{2/3}} k^{-5/3}, \quad (3)$$

where K^\pm are Kolmogorov's constants for MHD. Equation (3) was first derived by Marsch.¹⁵

The energy spectrum of the solar wind, a well-known observational platform for MHD turbulence, is closer to $k^{-5/3}$ than to $k^{-3/2}$.^{16,17} In addition, recent numerical^{18–20} and theoretical^{10,21,22} work support Kolmogorov-like phenomenology for MHD turbulence. Curiously, Kolmogorov's spectrum is observed, even in the presence of a mean magnetic field. To understand this theoretically, Verma,¹⁰ Sridhar and Goldreich,²¹ and Goldreich and Sridhar²² applied field theoretic techniques to MHD turbulence. Verma¹⁰ showed that the mean magnetic field B_0 responsible for the Alfvén

^{a)}Electronic mail: mkv@iitk.ac.in

effect becomes renormalized in strong turbulence [$B_0(k) \propto k^{-1/3}$]. When we substitute the renormalized B_0 in Eq. (1), the energy spectrum turns out to be proportional to $k^{-5/3}$. Sridhar and Goldreich,²¹ and Goldreich and Sridhar²² used a wave interaction picture and showed that the energy spectrum is anisotropic, and that it follows Kolmogorov's power law for strong turbulence.

In this paper we calculate the renormalized viscosity and resistivity for MHD. Here we test whether Kolmogorov's spectrum is a consistent solution of RG or not, if the turbulence is forced at large scale. We carry out wave number elimination and obtain recursive RG equations. Kolmogorov's spectrum is substituted for the correlation function in the recursive RG equation. After that we attempt to obtain a convergent solution for the renormalized viscosity and resistivity. If the convergent solution exists, then the Kolmogorov's spectrum is one of the correct choices for the energy spectrum of MHD turbulence. For these cases we compute many important quantities, e.g., renormalized viscosity, renormalized resistivity, cascade rates, etc., in a reasonably simple manner. In this paper we report the calculation of renormalized viscosity and resistivity, and in the subsequent paper (referred to as paper II) we will report the cascade rate calculation.

There are two field variables in MHD: the velocity fluctuation \mathbf{u} and the magnetic field fluctuation \mathbf{b} . The quantities of interest are kinetic energy (KE), magnetic energy (ME), total energy (KE+ME), and cross helicity ($H_c = \mathbf{u} \cdot \mathbf{b}$). The dimensionless parameters used in this paper are the ratio of twice the cross helicity and the total energy, called the normalized cross helicity σ_c [$\sigma_c = 2H_c / (KE + ME)$], and the ratio of KE and ME, called the Alfvén ratio r_A . In this paper we have assumed that the mean magnetic field is zero, and so are magnetic and kinetic helicities, i.e., we are considering nonhelical plasma. The calculation of the renormalized parameters is quite complex for arbitrary σ_c and r_A . Therefore, we limit ourselves to two limiting cases: (1) $\sigma_c = 0$ and whole range of r_A ; (2) $\sigma_c \rightarrow 1$ and $r_A = 1$. Even though a full range of σ_c is observed in terrestrial and extraterrestrial plasmas, the case $\sigma_c \approx 0$ is most pronounced.

The outline of the paper is as follows: in Secs. II and III we compute the renormalized viscosity and resistivity for the cases $\sigma_c = 0$ and $\sigma_c \rightarrow 1$, respectively. Section IV contains the summary and conclusions.

II. RG CALCULATION: $\sigma_c = 0$

In this section we will calculate the renormalized viscosity and resistivity of MHD equations for zero mean magnetic field and zero cross helicity ($\sigma_c = 0$). In this case, the RG equations in terms of velocity and magnetic field variables are simpler as compared to those with Elsässer variables. Therefore, we will work with \mathbf{u} and \mathbf{b} variables. We take the following form of the Kolmogorov's spectrum for KE [$E^u(k)$] and ME [$E^b(k)$]:

$$E^u(k) = K^u \Pi^{2/3} k^{-5/3}, \quad (4)$$

$$E^b(k) = E^u(k) / r_A, \quad (5)$$

where K^u is Kolmogorov's constant for MHD turbulence, and Π is the total energy flux. In the limit $\sigma_c = 0$, we have $E^+ = E^-$ and $\Pi^+ = \Pi^- = \Pi$ [cf. Eq. (3)]. Therefore, $E_{\text{total}}(k) = E^+(k) = E^u(k) + E^b(k)$ and

$$K^+ = K^u(1 + r_A^{-1}). \quad (6)$$

With these preliminaries we start our RG calculation. The incompressible MHD equations in the Fourier space are

$$\begin{aligned} (-i\omega + \nu k^2) u_i(\hat{k}) &= -\frac{i}{2} P_{ijm}^+(\mathbf{k}) \int d\hat{p} [u_j(\hat{p}) u_m(\hat{k} - \hat{p}) \\ &\quad - b_j(\hat{p}) b_m(\hat{k} - \hat{p})], \end{aligned} \quad (7)$$

$$(-i\omega + \eta k^2) b_i(\hat{k}) = -i P_{ijm}^-(\mathbf{k}) \int d\hat{p} [u_j(\hat{p}) b_m(\hat{k} - \hat{p})], \quad (8)$$

$$k_i u_i(\mathbf{k}) = 0, \quad (9)$$

$$k_i b_i(\mathbf{k}) = 0, \quad (10)$$

with

$$P_{ijm}^+(\mathbf{k}) = k_j P_{im}(\mathbf{k}) + k_m P_{ij}(\mathbf{k}); \quad (11)$$

$$P_{im}(\mathbf{k}) = \delta_{im} - \frac{k_i k_m}{k^2}; \quad (12)$$

$$P_{ijm}^-(\mathbf{k}) = k_j \delta_{im} - k_m \delta_{ij}; \quad (13)$$

$$\hat{k} = (\mathbf{k}, \omega); \quad (14)$$

$$d\hat{p} = d\mathbf{p} d\omega / (2\pi)^{d+1}. \quad (15)$$

Here ν and η are the viscosity and the resistivity, respectively, and d is the space dimension.

In our RG procedure the wave number range (k_N, k_0) is divided logarithmically into N shells. The n th shell is (k_n, k_{n-1}) , where $k_n = h^n k_0$ ($h < 1$). In the following discussion, we carry out the elimination of the first shell (k_1, k_0) and obtain the modified MHD equations. We then proceed iteratively to eliminate higher shells and get a general expression for the modified MHD equations. The renormalization group procedure is as follows.

(1) We divide the spectral space into two parts: (1) the shell $(k_1, k_0) = k^>$, which is to be eliminated; (2) $(k_N, k_1) = k^<$; set of modes to be retained. Note that ν_0 and η_0 denote the viscosity and resistivity before the elimination of the first shell.

(2) We rewrite Eqs. (7) and (8) for $k^<$ and $k^>$. The equations for $u_i^<(\hat{k})$ and $b_i^<(\hat{k})$ modes are

$$\begin{aligned} [-i\omega + \Sigma_{(0)}^{uu}(k)] u_i^<(\hat{k}) + \Sigma_{(0)}^{ub}(k) b_i^<(\hat{k}) &= -\frac{i}{2} P_{ijm}^+(\mathbf{k}) \int d\hat{p} \{ [u_j^<(\hat{p}) u_m^<(\hat{k} - \hat{p})] \\ &\quad + 2[u_j^<(\hat{p}) u_m^>(\hat{k} - \hat{p})] + [u_j^>(\hat{p}) u_m^>(\hat{k} - \hat{p})] \\ &\quad - \text{similar terms for } b\}; \end{aligned} \quad (16)$$

$$\begin{aligned}
 & [-i\omega + \Sigma_{(0)}^{bb}(k)]b_i^<(\hat{k}) + \Sigma_{(0)}^{bu}(k)u_i^<(\hat{k}) \\
 &= -iP_{ijm}^-(\mathbf{k}) \int d\hat{p} \{ [u_j^<(\hat{p})b_m^<(\hat{k}-\hat{p})] \\
 &+ [u_j^<(\hat{p})b_m^>(\hat{k}-\hat{p}) + u_j^>(\hat{p})b_m^<(\hat{k}-\hat{p})] \\
 &+ [u_j^>(\hat{p})b_m^>(\hat{k}-\hat{p})] \}. \quad (17)
 \end{aligned}$$

The Σ 's appearing in the equations are usually called the ‘‘self-energy’’ in quantum field theory language. In the first iteration, $\Sigma_{(0)}^{uu} = \nu_{(0)}k^2$ and $\Sigma_{(0)}^{bb} = \eta_{(0)}k^2$, while the other two Σ 's are zero. The equation for $u_i^<(\hat{k})$ modes can be obtained by interchanging $<$ and $>$ in the above equations.

The terms given in the second and third brackets on the right-hand side of Eqs. (16), (17) are calculated perturbatively. Since we are interested in the statistical properties of \mathbf{u} and \mathbf{b} fluctuations, we perform the usual ensemble average of the system.⁴ We assume that $\mathbf{u}^>(\hat{k})$ and $\mathbf{b}^>(\hat{k})$ have Gaussian distributions with zero mean, while $\mathbf{u}^<(\hat{k})$ and $\mathbf{b}^<(\hat{k})$ are unaffected by the averaging process. Hence,

$$\langle u_i^>(\hat{k}) \rangle = 0, \quad (18)$$

$$\langle b_i^>(\hat{k}) \rangle = 0, \quad (19)$$

$$\langle u_i^<(\hat{k}) \rangle = u_i^<(\hat{k}), \quad (20)$$

$$\langle b_i^<(\hat{k}) \rangle = b_i^<(\hat{k}), \quad (21)$$

and

$$\langle u_i^>(\hat{p})u_j^>(\hat{q}) \rangle = P_{ij}(\mathbf{p})C^{uu}(\hat{p})\delta(\hat{p}+\hat{q}), \quad (22)$$

$$\langle b_i^>(\hat{p})b_j^>(\hat{q}) \rangle = P_{ij}(\mathbf{p})C^{bb}(\hat{p})\delta(\hat{p}+\hat{q}), \quad (23)$$

$$\langle u_i^>(\hat{p})b_j^>(\hat{q}) \rangle = P_{ij}(\mathbf{p})C^{ub}(\hat{p})\delta(\hat{p}+\hat{q}). \quad (24)$$

The triple-order correlations $\langle X_i^>(\hat{k})X_j^>(\hat{p})X_m^>(\hat{q}) \rangle$ are zero due to the Gaussian nature of the fluctuations. Here, X stands for u or b . In addition, we also neglect the contribution from the triple nonlinearity $\langle X_i^<(\hat{k})X_j^<(\hat{p})X_m^<(\hat{q}) \rangle$. The last assumption is used in many of the turbulence RG calculations.^{4,5} Refer to Zhou and Vahala²³ for a discussion on the importance of the triple nonlinearity.

The details of the perturbative calculation is given in Appendix A. To the first order, the second bracketed terms of Eqs. (16), (17) vanish, but the nonvanishing third bracketed terms yield corrections to Σ 's. Equations (16), (17) can now be approximated by

$$\begin{aligned}
 & (-i\omega + \Sigma_{(0)}^{uu} + \delta\Sigma_{(0)}^{uu})u_i^<(\hat{k}) + (\Sigma_{(0)}^{ub} + \delta\Sigma_{(0)}^{ub})b_i^<(\hat{k}) \\
 &= -\frac{i}{2}P_{ijm}^+(\mathbf{k}) \int d\hat{p} [u_j^<(\hat{p})u_m^<(\hat{k}-\hat{p}) \\
 &- b_j^<(\hat{p})b_m^<(\hat{k}-\hat{p})], \quad (25)
 \end{aligned}$$

$$\begin{aligned}
 & (-i\omega + \Sigma_{(0)}^{bb} + \delta\Sigma_{(0)}^{bb})b_i^<(\hat{k}) + (\Sigma_{(0)}^{bu} + \delta\Sigma_{(0)}^{bu})u_i^<(\hat{k}) \\
 &= -iP_{ijm}^-(\mathbf{k}) \int d\hat{p} [u_j^<(\hat{p})b_m^<(\hat{k}-\hat{p})], \quad (26)
 \end{aligned}$$

with

$$\begin{aligned}
 \delta\Sigma_{(0)}^{uu}(k) &= \frac{1}{(d-1)k^2} \int_{\hat{p}+\hat{q}=k}^{\Delta} d\hat{p} \\
 &\times [S(k,p,q)G^{uu}(\hat{p})C^{uu}(\hat{q}) \\
 &- S_6(k,p,q)G^{bb}(\hat{p})C^{bb}(\hat{q}) \\
 &+ S_6(k,p,q)G^{ub}(\hat{p})C^{ub}(\hat{q}) \\
 &- S(k,p,q)G^{bu}(\hat{p})C^{ub}(\hat{q})], \quad (27)
 \end{aligned}$$

$$\begin{aligned}
 \delta\Sigma_{(0)}^{ub}(k) &= \frac{1}{(d-1)k^2} \int_{\hat{p}+\hat{q}=k}^{\Delta} d\hat{p} \\
 &\times [-S(k,p,q)G^{uu}(\hat{p})C^{ub}(\hat{q}) \\
 &+ S_5(k,p,q)G^{ub}(\hat{p})C^{uu}(\hat{q}) \\
 &+ S(k,p,q)G^{bu}(\hat{p})C^{bb}(\hat{q}) \\
 &- S_5(k,p,q)G^{bb}(\hat{p})C^{ub}(\hat{q})], \quad (28)
 \end{aligned}$$

$$\begin{aligned}
 \delta\Sigma_{(0)}^{bu}(k) &= \frac{1}{(d-1)k^2} \int_{\hat{p}+\hat{q}=k}^{\Delta} d\hat{p} \\
 &\times [S_8(k,p,q)G^{uu}(\hat{p})C^{ub}(\hat{q}) \\
 &+ S_{10}(k,p,q)G^{bb}(\hat{p})C^{ub}(\hat{q}) \\
 &+ S_{12}(k,p,q)G^{ub}(\hat{p})C^{bb}(\hat{q}) \\
 &- S_7(k,p,q)G^{bu}(\hat{p})C^{uu}(\hat{q})], \quad (29)
 \end{aligned}$$

$$\begin{aligned}
 \delta\Sigma_{(0)}^{bb}(k) &= \frac{1}{(d-1)k^2} \int_{\hat{p}+\hat{q}=k}^{\Delta} d\hat{p} \\
 &\times [-S_8(k,p,q)G^{uu}(\hat{p})C^{bb}(\hat{q}) \\
 &+ S_9(k,p,q)G^{bb}(\hat{p})C^{uu}(\hat{q}) \\
 &+ S_{11}(k,p,q)G^{ub}(\hat{p})C^{ub}(\hat{q}) \\
 &- S_9(k,p,q)G^{bu}(\hat{p})C^{ub}(\hat{q})]. \quad (30)
 \end{aligned}$$

The quantities $S_i(k,p,q)$ are given in Appendix B. The integral Δ is to be done over the first shell.

The full-fledged calculation of the Σ 's is quite involved. Therefore, we take two special cases: (1) $C^{ub}=0$ or $\sigma_c=0$; and (2) $C^{ub} \approx C^{uu} \approx C^{bb}$ or $\sigma_c \rightarrow 1$. In this section we will discuss only the case $\sigma_c=0$. The other case will be taken up in the next section. A word of caution is in order here. In our calculation the parameters used are $\sigma_c(k) = 2C^{ub}(k)/[C^{uu}(k)+C^{bb}(k)]$ and $r_A(k) = E^u(k)/E^b(k)$. These parameters differ from the global σ_c and r_A , yet we have restricted ourselves to the limiting cases of constant $\sigma_c(k)$ and $r_A(k)$ because of simplicity.

When $\sigma_c=0$, an inspection of the self-energy diagrams shows that $\Sigma^{ub} = \Sigma^{bu} = 0$, and $G^{ub} = G^{bu} = 0$. Clearly, the equations become much simpler because of the diagonal nature of matrices G and Σ . The two quantities of interest $\delta\Sigma_{(0)}^{uu}$ and $\delta\Sigma_{(0)}^{bb}$ will be given by

$$\begin{aligned}
 \delta\Sigma_{(0)}^{uu}(\hat{k}) &= \frac{1}{d-1} \int_{\hat{p}+\hat{q}=k}^{\Delta} d\hat{p} [S(k,p,q)G^{uu}(p)C^{uu}(q) \\
 &- S_6(k,p,q)G^{bb}(p)C^{bb}(q)], \quad (31)
 \end{aligned}$$

$$\delta\Sigma^{bb}(\hat{k}) = \frac{1}{d-1} \int_{\hat{p}+\hat{q}=\hat{k}}^{\Delta} d\hat{p} [-S_8(k,p,q)G^{uu}(p)C^{bb}(q) + S_9(k,p,q)G^{bb}(p)C^{uu}(q)]. \quad (32)$$

The expressions for $\delta\Sigma$'s involve correlation functions and the Green's function, which are themselves functions of Σ 's. In earlier RG calculations (see, e.g., Refs. 1, 4) the correlation function $C(\hat{k})$ is function of the forcing noise spectrum. In our self-consistent scheme we assume that we are in the inertial range, and the energy spectrum is proportional to Kolmogorov's $\frac{5}{3}$ power law. After that the renormalized Green's function, or renormalized ν , is computed iteratively.

The frequency dependence of the correlation function are taken as $C^{uu}(k, \omega) = 2C^{uu}(k)\Re[G^{uu}(k, \omega)]$ and $C^{bb}(k, \omega) = 2C^{bb}(k)\Re[G^{bb}(k, \omega)]$. In other words, the relaxation time scale of the correlation function is assumed to be the same as that of the corresponding Green's function. Since we are interested in the large time-scale behavior of turbulence, we take the limit ω going to zero. Under these assumptions, the above equations become

$$\delta\nu_{(0)}(k) = \frac{1}{(d-1)k^2} \int_{\mathbf{p}+\mathbf{q}=\mathbf{k}}^{\Delta} \frac{d\mathbf{p}}{(2\pi)^d} \times \left(S(k,p,q) \frac{C^{uu}(q)}{\nu_{(0)}(p)p^2 + \nu_{(0)}(q)q^2} - S_6(k,p,q) \frac{C^{bb}(q)}{\eta_{(0)}(p)p^2 + \eta_{(0)}(q)q^2} \right), \quad (33)$$

$$\delta\eta_{(0)}(k) = \frac{1}{(d-1)k^2} \int_{\mathbf{p}+\mathbf{q}=\mathbf{k}}^{\Delta} \frac{d\mathbf{p}}{(2\pi)^d} \times \left(-S_9(k,p,q) \frac{C^{bb}(q)}{\nu_{(0)}(p)p^2 + \eta_{(0)}(q)q^2} + S_9(k,p,q) \frac{C^{uu}(q)}{\eta_{(0)}(p)p^2 + \nu_{(0)}(q)q^2} \right). \quad (34)$$

Note that $\nu(k) = \Sigma^{uu}(k)/k^2$ and $\eta(k) = \Sigma^{bb}(k)/k^2$.

There are some important points to remember in the above step. The frequency integral in the above is done using a contour integral. It can be shown that the integrals are nonzero only when both the components appearing the denominator are of the same sign. For example, the first term of Eq. (34) is nonzero only when both $\nu_{(0)}(p)$ and $\eta_{(0)}(q)$ are of the same sign.

Let us denote $\nu_{(1)}(k)$ and $\eta_{(1)}(k)$ as the renormalized viscosity and resistivity, respectively, after the first step of wave number elimination. Hence,

$$\nu_{(1)}(k) = \nu_{(0)}(k) + \delta\nu_{(0)}(k); \quad (35)$$

$$\eta_{(1)}(k) = \eta_{(0)}(k) + \delta\eta_{(0)}(k). \quad (36)$$

We keep eliminating the shells one after the other by the above procedure. After $n+1$ iterations we obtain

$$\nu_{(n+1)}(k) = \nu_{(n)}(k) + \delta\nu_{(n)}(k), \quad (37)$$

$$\eta_{(n+1)}(k) = \eta_{(n)}(k) + \delta\eta_{(n)}(k), \quad (38)$$

where the equations for $\delta\nu_{(n)}(k)$ and $\delta\eta_{(n)}(k)$ are the same as Eqs. (33), (34), except that $\nu_{(0)}(k)$ and $\eta_{(0)}(k)$ appearing in the equations are to be replaced by $\nu_{(n)}(k)$ and $\eta_{(n)}(k)$, respectively. Clearly $\nu_{(n+1)}(k)$ and $\eta_{(n+1)}(k)$ are the renormalized viscosity and resistivity after the elimination of the $(n+1)$ th shell.

We need to compute $\delta\nu_{(n)}$ and $\delta\eta_{(n)}$ for various n . These computations, however, require $\nu_{(n)}$ and $\eta_{(n)}$. In our scheme we solve these equations iteratively. In Eqs. (33), (34) we substitute $C(k)$ by the one-dimensional energy spectrum $E(k)$,

$$C^{uu}(k) = \frac{2(2\pi)^d}{S_d(d-1)} k^{-(d-1)} E^u(k), \quad (39)$$

$$C^{bb}(k) = \frac{2(2\pi)^d}{S_d(d-1)} k^{-(d-1)} E^b(k), \quad (40)$$

where S_d is the surface area of d -dimensional spheres. We assume that $E^u(k)$ and $E^b(k)$ follow Eqs. (4), (5), respectively. Regarding $\nu_{(n)}$ and $\eta_{(n)}$, we attempt the following form of a solution:

$$\nu_{(n)}(k_n k') = (K^u)^{1/2} \Pi^{1/3} k_n^{-4/3} \nu_{(n)}^*(k'), \quad (41)$$

$$\eta_{(n)}(k_n k') = (K^u)^{1/2} \Pi^{1/3} k_n^{-4/3} \eta_{(n)}^*(k'), \quad (42)$$

with $k = k_{n+1} k'$ ($k' < 1$). We expect $\nu_{(n)}^*(k')$ and $\eta_{(n)}^*(k')$ to be universal functions for large n . The substitution of $C^{uu}(k)$, $C^{bb}(k)$, $\nu_{(n)}(k)$, and $\eta_{(n)}(k)$ yields the following equations:

$$\delta\nu_{(n)}^*(k') = \frac{1}{(d-1)} \int_{\mathbf{p}'+\mathbf{q}'=\mathbf{k}'} d\mathbf{q}' \frac{2}{(d-1)S_d} \frac{E^u(q')}{q'^{d-1}} \times \left(S(k',p',q') \frac{1}{\nu_{(n)}^*(hp')p'^2 + \nu_{(n)}^*(hq')q'^2} - S_6(k',p',q') \frac{r_A^{-1}}{\eta_{(n)}^*(hp')p'^2 + \eta_{(n)}^*(hq')q'^2} \right), \quad (43)$$

$$\delta\eta_{(n)}^*(k') = \frac{1}{(d-1)} \int_{\mathbf{p}'+\mathbf{q}'=\mathbf{k}'} d\mathbf{q}' \frac{2}{(d-1)S_d} \frac{E^u(q')}{q'^{d-1}} \times \left(-S_8(k',p',q') \frac{1}{\nu_{(n)}^*(hp')p'^2 + \eta_{(n)}^*(hq')q'^2} + S_9(k',p',q') \frac{r_A^{-1}}{\eta_{(n)}^*(hp')p'^2 + \nu_{(n)}^*(hq')q'^2} \right), \quad (44)$$

$$\nu_{(n+1)}^*(k') = h^{4/3} \nu_{(n)}^*(hk') + h^{-4/3} \delta\nu_{(n)}^*(k'), \quad (45)$$

$$\eta_{(n+1)}^*(k') = h^{4/3} \eta_{(n)}^*(hk') + h^{-4/3} \delta\eta_{(n)}^*(k'), \quad (46)$$

where the integrals in the above equations are performed iteratively over a region $1 \leq p', q' \leq 1/h$ with the constraint that $\mathbf{p}'+\mathbf{q}'=\mathbf{k}'$. Fournier and Frisch³ showed the above volume integral in d dimensions to be

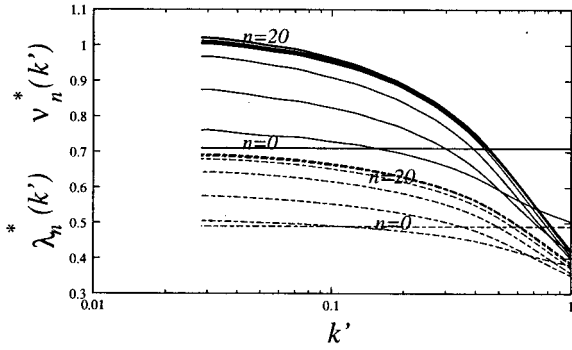


FIG. 1. The plot of $\nu^*(k')$ (solid) and $\eta^*(k')$ (dashed) vs k' for $d=3$ and $\sigma_c=0, r_A=1$. Values at various iterations are shown by different curves.

$$\int_{\mathbf{p}'+\mathbf{q}'=\mathbf{k}'} d\mathbf{q}' = S_{d-1} \int dp dq \left(\frac{pq}{k}\right)^{d-2} (\sin \alpha)^{d-3}, \quad (47)$$

where α is the angle between vectors \mathbf{p} and \mathbf{q} .

Now we solve the above four equations self-consistently for various r_A 's. We have taken $h=0.7$. We start with constant values of $\nu_{(0)}^*$ and $\eta_{(0)}^*$ and compute the integrals using the Gauss quadrature technique. Once $\delta\nu_{(0)}^*$ and $\delta\eta_{(0)}^*$ have been computed, we can calculate $\nu_{(1)}^*$ and $\eta_{(1)}^*$. We iterate this process until $\nu_{(m+1)}^*(k') \approx \nu_{(m)}^*(k')$ and $\eta_{(m+1)}^*(k') \approx \eta_{(m)}^*(k')$, that is, until they converge. We have reported the limiting ν^* and η^* whenever the solution converges. The criterion for convergence is that the error must be less than 1%. This criterion is usually achieved by $n=10$ or so. The result of our RG analysis is given below.

We have carried out the RG analysis for various space dimensions and find that the solution converges for all $d > d_c \approx 2.2$. Hence, the RG fixed point for MHD turbulence is stable for $d \geq d_c$. For illustration of the convergent solution, see Fig. 1 for the plots of $\nu_{(n)}^*(k')$ and $\eta_{(n)}^*(k')$ for $d=3, r_A=1$. The RG fixed point for $d < d_c$ is unstable. Refer to the plots of Fig. 2 for $d=2, r_A=1$ as an example of an unstable solution. From this observation we can claim that Kolmogorov's power law is a consistent solution of MHD RG equations, at least for $d \geq d_c$. The values of asymptotic ($k' \rightarrow 0$ limit) ν^* and η^* for various d and $r_A=1$ are displayed in Table I. Clearly ν^* and η^* decreases with the increase in d for $d \geq 4$. The plot of Fig. 3 shows that both ν^* and η^* are

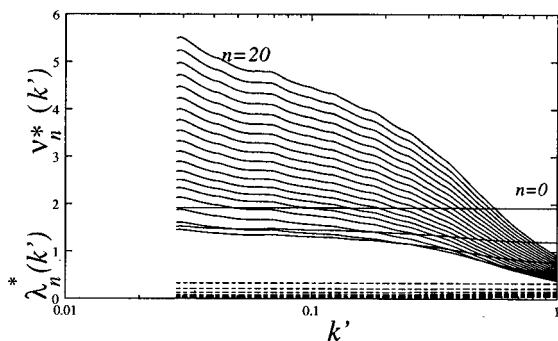


FIG. 2. The plot of $\nu^*(k')$ and $\eta^*(k')$ vs k' for $d=2$ and $\sigma_c=0, r_A=1$.

TABLE I. The values of $\nu^*, \eta^*, \nu^{uu*}, \nu^{ub*}, \eta^{bu*}, \eta^{bb*}$ for various space dimensions d with $r_A=1$ and $\sigma_c=0$.

d	ν^*	η^*	Pr	ν^{uu*}	ν^{ub*}	η^{bu*}	η^{bb*}
2.1
2.2	1.9	0.32	6.0	-0.041	1.96	-0.44	0.76
2.5	1.2	0.57	2.1	0.089	1.15	-0.15	0.72
3.0	1.00	0.69	1.4	0.20	0.80	0.078	0.61
4.0	0.83	0.70	1.2	0.27	0.56	0.21	0.49
7.0	0.62	0.59	1.1	0.26	0.36	0.25	0.34
10.0	0.51	0.50	1.0	0.23	0.28	0.22	0.28
50.0	0.23	0.23	1.0	0.11	0.12	0.11	0.12
100	0.14	0.14	1.0	0.065	0.069	0.066	0.069

proportional to $d^{-1/2}$. In the same plot we have also displayed ν^* for pure fluid turbulence; there too $\nu^* \propto d^{-1/2}$. This result is consistent with the Fournier *et al.* prediction for fluid turbulence.²⁴

An important point to note is that the stability of the RG fixed point in a given space dimension depends on the Alfvén ratio and normalized cross helicity. For example, for $d=2.2$ the RG fixed point is stable for $r_A \geq 1$, but unstable for $r_A < 1$. A detailed study of stability of the RG fixed point is required to ascertain the boundary of stability.

The values of renormalized parameters for $d=3$ and various r_A are shown in Table II. For large r_A (fluid-dominated regime), ν^* is close to renormalized viscosity of fluid turbulence ($r_A = \infty$), but η^* is also finite. That means there is a positive magnetic energy flux, even when $r_A \rightarrow \infty$. As r_A is decreased, η^* decreases but ν^* increases, or the Prandtl number $\text{Pr} = \nu/\eta$ increases. This trend is seen until $r_A \approx 0.25$, where the RG fixed point with nonzero ν^* and η^* becomes unstable, and the trivial RG fixed point with $\nu^* = \eta^* = 0$ becomes stable. This result suggests an absence of turbulence for r_A below 0.25 (approximately). Note that in the $r_A \rightarrow 0$ (fully magnetic) limit, the MHD equations become linear, hence there is no turbulence. Surprisingly, our RG calculation suggests that turbulence disappear near $r_A = 0.25$ itself.

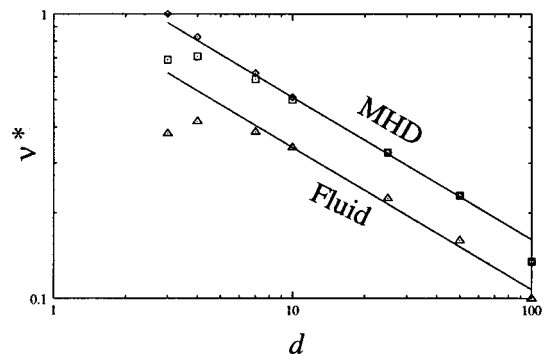


FIG. 3. The plot of asymptotic ν^* (square) and η^* (diamond) vs d for $\sigma_c=0$ and $r_A=1$. The fluid ν^* (triangle) is also plotted for reference. The solid lines are the $d^{-1/2}$ curves.

TABLE II. The values of ν^* , η^* , ν^{uu^*} , ν^{ub^*} , η^{bu^*} , η^{bb^*} for various r_A when $d=3$ and $\sigma_c=0$.

r_A	ν^*	η^*	Pr	ν^{uu^*}	ν^{ub^*}	η^{bu^*}	η^{bb^*}
∞	0.38	0.38
5000	0.36	0.85	0.42	0.36	$1.4E-4$	-0.023	0.87
100	0.36	0.85	0.42	0.36	$7.3E-3$	-0.022	0.87
5	0.47	0.82	0.57	0.32	0.15	$-4.7E-4$	0.82
2	0.65	0.78	0.83	0.27	0.38	0.031	0.75
1	1.00	0.69	1.4	0.20	0.80	0.078	0.61
0.5	2.1	0.50	4.2	0.11	2.00	0.15	0.35
0.3	11.0	0.14	78	0.022	11.0	0.082	0.053
0.2

The final $\nu^*(k')$ and $\eta^*(k')$ are constant for small k' but shifts toward zero for larger k' (see Fig. 1). Similar behavior has been seen by McComb and co-workers²⁵ for fluid turbulence; this behavior is attributed to the neglect of triple nonlinearity, and the corrective procedure has been prescribed by Zhou and Vahala.²³ For simplicity, we have not included the effects of triple nonlinearity in our calculation.

Kraichnan's $k^{-3/2}$ energy spectrum [see Eq. (1)] and $\sigma^{uu} = \sigma^{bb} \propto k B_0$ do not satisfy the RG equations. This implies that Kraichnan's $3/2$ power law is not a consistent solution of RG equations.

Pouquet²⁶ and Ishizawa and Hattori²⁷ calculated the contributions to the renormalized (eddy) viscosity and resistivity from each of the four nonlinear terms of MHD equations using an EDQNM (eddy-damped-quasi-normal-Markovian) approximation. This calculation has been done for $d=2$. Let us denote the quantities ν^{uu} , ν^{ub} , η^{bu} , η^{bb} as contributions from the terms $\mathbf{u} \cdot \nabla \mathbf{u}$, $-\mathbf{b} \cdot \nabla \mathbf{b}$, $-\mathbf{u} \cdot \nabla \mathbf{b}$, $\mathbf{b} \cdot \nabla \mathbf{u}$, respectively. Note that various cascade rates of MHD turbulence²⁷⁻²⁹ can be inferred from these parameters. The cascade rate from inside of the X sphere ($X <$) to outside of the Y sphere ($Y >$) is

$$\Pi_{Y>}^{X<} = \int_0^{k_N} 2\nu^{XY}(k)k^2 E^X(k)dk, \quad (48)$$

where X, Y denote u or b . We have computed ν^{XY} for $d \geq d_c$; their values are listed in Tables I and II. Our results show that η^{bb} is positive. Pouquet argues that η^{bb} is negative, while Ishizawa finds it to be positive. Since our RG procedure is applicable only for $d > d_c = 2.2$, it is not proper to compare our results with those of Pouquet²⁶ and Ishizawa and Hattori.²⁷ However, we can claim that the magnetic energy cascade rate ($\Pi_{b>}^{b<}$) is positive for all $d > d_c$ because $\eta^{bb} > 0$.

The eddy viscosity and resistivity listed in Table I shows that η^{bb^*} and ν^{ub^*} decrease as d increases. On the contrary, η^{bu^*} and ν^{uu^*} first increases, until around $d=5$ then decreases as d increases. Since MHD fluxes are proportional to these parameters, the corresponding fluxes decrease as d is increased beyond 5. Near $d=2$, ν^{uu^*} is negative, reminiscent of inverse cascade energy in two-dimensional fluid turbulence in the $\frac{5}{3}$ region. Also, η^{bu^*} is negative near $d=2$, i.e., there is a negative energy cascade from the b sphere to outside the u sphere. The above results are consistent with the

recent simulation results of Dar *et al.*²⁹ on two-dimensional MHD turbulence.

The variation of ν^{XY^*} with r_A for $d=3$ is displayed in Table II. For large r_A , ν^{uu^*} is close to the fluid turbulence ν^* . However, η^{bb^*} also finite. Hence, there is a significant magnetic energy cascade to inside of the b sphere to outside of the b sphere even in the fluid-dominated case. As r_A is decreased, ν^{ub^*} and η^{bu^*} increase; hence cascade rates from the u sphere to outside the b sphere, and the b sphere to outside the u sphere start becoming important. Incidentally, both ν^{uu^*} and η^{bb^*} decrease as r_A decreases.

In this section we have calculated the renormalized viscosity and resistivity for $\sigma_c=0$. In the next section we will calculate these parameters for the $\sigma_c \rightarrow 1$ limit.

III. RG CALCULATION: $\sigma_c \rightarrow 1$

The \mathbf{u} and \mathbf{b} correlation is very high when $\sigma_c \rightarrow 1$. For this case it is best to work with Elsässer variables $\mathbf{z}^\pm = \mathbf{u} \pm \mathbf{b}$. In terms of Elsässer variables, $\langle |z^+|^2 \rangle \gg \langle |z^-|^2 \rangle$ when $\sigma_c \rightarrow 1$. These types of fluctuations have been observed in the solar wind near the Sun. However, by the time the solar wind approaches the Earth, the normalized cross helicity is close to zero.

In this section we will briefly discuss the RG treatment for the above case. For the following discussion we will denote $\langle |z^-|^2 \rangle / \langle |z^+|^2 \rangle = r = (1 - \sigma_c) / (1 + \sigma_c)$. Clearly $r \ll 1$.

MHD equations in terms of Elsässer variables are

$$\begin{aligned} & (-i\omega + \nu_{(0)\pm\pm} k^2) z_i^\pm(\hat{k}) + \nu_{(0)\pm\mp} k^2 z_i^\mp(\hat{k}) \\ & = -iM_{ijm}(\mathbf{k}) \int d\hat{p} [z_j^\mp(\hat{p}) z_m^\pm(\hat{k}-\hat{p})], \end{aligned} \quad (49)$$

where

$$M_{ijm}(\mathbf{k}) = k_j P_{im}(\mathbf{k}). \quad (50)$$

Note that the above equations contain four dissipative coefficients $\nu_{\pm\pm}$ and $\nu_{\pm\mp}$ instead of the usual two constants $\nu_\pm = (\nu \pm \eta)/2$. This is because $+-$ symmetry is broken in this case; consequently RG generates the other two constants. We carry out the same procedure as outlined in the previous section. After $n+1$ steps of the RG calculation, the above equations become

$$\begin{aligned} & [-i\omega \mp [\nu_{(n)\pm\pm}(k) + \delta\nu_{(n)\pm\pm}(k)]k^2] z_i^\pm(\hat{k}) \\ & + [\nu_{(n)\pm\mp}(k) + \delta\nu_{(n)\pm\mp}(k)]k^2 z_i^\mp(\hat{k}) \\ & = -iM_{ijm}(\mathbf{k}) \int d\hat{p} z_j^\mp(\hat{p}) z_m^\pm(\hat{k}-\hat{p}), \end{aligned} \quad (51)$$

with

$$\begin{aligned} \delta\nu_{(n)++}(k) & = \frac{1}{(d-1)k^2} \int_{\hat{p}+\hat{q}=\hat{k}}^\Delta d\hat{p} \\ & \times [S_1(k, p, q) G_{(n)}^{++}(\hat{p}) C^{--}(\hat{q}) \\ & + S_2(k, p, q) G_{(n)}^{+-}(\hat{p}) C^{--}(\hat{q}) \\ & + S_3(k, p, q) G_{(n)}^{-+}(\hat{p}) C^{+-}(\hat{q}) \\ & + S_4(k, p, q) G_{(n)}^{--}(\hat{p}) C^{+-}(\hat{q})], \end{aligned} \quad (52)$$

$$\begin{aligned} \delta\nu_{(n)+-}(k) &= \frac{1}{(d-1)k^2} \int_{\hat{p}+\hat{q}=k}^{\Delta} d\hat{p} \\ &\times [S_1(k,p,q)G_{(n)}^{+-}(\hat{p})C^{-+}(\hat{q}) \\ &+ S_2(k,p,q)G_{(n)}^{++}(\hat{p})C^{-+}(\hat{q}) \\ &+ S_3(k,p,q)G_{(n)}^{--}(\hat{p})C^{++}(\hat{q}) \\ &+ S_4(k,p,q)G_{(n)}^{-+}(\hat{p})C^{++}(\hat{q})], \end{aligned} \quad (53)$$

where the integral is performed over the $(n+1)$ th shell (k_{n+1}, k_n) . The equations for the other two $\delta\nu$'s can be obtained by interchanging $+$ and $-$ signs. Now we assume that the Alfvén ratio is one, i.e., $C^{+-} = E^u - E^b = 0$. Under this condition, the above equations reduce to

$$\begin{aligned} \delta\nu_{(n)++}(k) &= \frac{1}{(d-1)k^2} \int_{\hat{p}+\hat{q}=k}^{\Delta} d\hat{p} [S_1(k,p,q)G_{(n)}^{++}(\hat{p}) \\ &+ S_2(k,p,q)G_{(n)}^{+-}(\hat{p})]C^{--}(\hat{q}), \end{aligned} \quad (54)$$

$$\begin{aligned} \delta\nu_{(n)+-}(k) &= \frac{1}{(d-1)k^2} \int_{\hat{p}+\hat{q}=k}^{\Delta} d\hat{p} [S_3(k,p,q)G_{(n)}^{--}(\hat{p}) \\ &+ S_4(k,p,q)G_{(n)}^{-+}(\hat{p})]C^{++}(\hat{q}), \end{aligned} \quad (55)$$

$$\begin{aligned} \delta\nu_{(n)-+}(k) &= \frac{1}{(d-1)k^2} \int_{\hat{p}+\hat{q}=k}^{\Delta} d\hat{p} [S_3(k,p,q)G_{(n)}^{++}(\hat{p}) \\ &+ S_4(k,p,q)G_{(n)}^{+-}(\hat{p})]C^{--}(\hat{q}), \end{aligned} \quad (56)$$

$$\begin{aligned} \delta\nu_{(n)--}(k) &= \frac{1}{(d-1)k^2} \int_{\hat{p}+\hat{q}=k}^{\Delta} d\hat{p} [S_1(k,p,q)G_{(n)}^{--}(\hat{p}) \\ &+ S_2(k,p,q)G_{(n)}^{-+}(\hat{p})]C^{++}(\hat{q}). \end{aligned} \quad (57)$$

The inspection of Eqs. (54)–(57) reveal that ν_{++} and ν_{--} are of the order of r . Hence, we take the $\hat{\nu}$ matrix to be of the form

$$\hat{\nu}(k, \omega) = \begin{pmatrix} r\zeta & \alpha \\ r\psi & \beta \end{pmatrix}. \quad (58)$$

It is convenient to transform the frequency integrals in Eqs. (54)–(57) into temporal integrals, which leads to

$$\begin{aligned} \delta\nu_{(n)++}(k) &= \frac{1}{(d-1)k^2} \int_{\mathbf{p}+\mathbf{q}=\mathbf{k}}^{\Delta} \frac{d\mathbf{p}}{(2\pi)^d} \\ &\times \int_{-\infty}^t dt' [S_1(k,p,q)G_{(n)}^{++}(\mathbf{p}, t-t') \\ &+ S_2(k,p,q)G_{(n)}^{+-}(\mathbf{p}, t-t')] \\ &\times C^{--}(\mathbf{q}, t-t'), \end{aligned} \quad (59)$$

and similar forms for equations for other ν 's. The Green's function $\hat{G}(k, t-t') = \exp[-\hat{\nu}k^2(t-t')]$ can be easily evaluated by diagonalizing the matrix $\hat{\nu}$. The final form of $\hat{G}(k, t-t')$ to leading order in r is

$$\hat{G}(k, t-t') = \begin{pmatrix} 1 - \frac{r\alpha\psi}{\beta^2}(1 - e^{-\beta(t-t')}) & -\left[\frac{\alpha}{\beta} + \frac{r\alpha}{\beta}\left(\frac{\zeta}{\beta} - \frac{2\alpha\psi}{\beta^2}\right)\right](1 - e^{-\beta(t-t')}) \\ -\frac{r\psi}{\beta}(1 - e^{-\beta(t-t')}) & e^{-\beta(t-t')} + \frac{r\alpha\psi}{\beta^2}(1 - e^{-\beta(t-t')}) \end{pmatrix}. \quad (60)$$

The correlation matrix $\hat{C}(k, t-t')$ is given by

$$\begin{pmatrix} C^{++}(k, t-t') & C^{+-}(k, t-t') \\ C^{-+}(k, t-t') & C^{--}(k, t-t') \end{pmatrix} = \hat{G}(k, t-t') \begin{pmatrix} C^{++}(k) & C^{+-}(k) \\ C^{-+}(k) & C^{--}(k) \end{pmatrix}. \quad (61)$$

The substitution of correlation functions and Green's functions yield the following expressions for the elements of $\delta\hat{\nu}$:

$$\begin{aligned} \delta\zeta_{(n)}(k) &= \frac{1}{(d-1)k^2} \int^{\Delta} \frac{d\mathbf{p}}{(2\pi)^d} C^+(q) \left[S_1(k,p,q) \frac{1}{\beta_{(n)}(q)q^2} + S_2(k,p,q) \frac{\alpha_{(n)}(p)}{\beta_{(n)}(p)} \left(\frac{1}{\beta_{(n)}(p)p^2 + \beta_{(n)}(q)q^2} - \frac{1}{\beta_{(n)}(q)q^2} \right) \right. \\ &\left. - S_3(k,p,q) \frac{\alpha_{(n)}(q)}{\beta_{(n)}(q)} \left(\frac{1}{\beta_{(n)}(p)p^2 + \beta_{(n)}(q)q^2} - \frac{1}{\beta_{(n)}(p)p^2} \right) \right], \end{aligned} \quad (62)$$

$$\delta\alpha_{(n)}(k) = \frac{1}{(d-1)k^2} \int^{\Delta} \frac{d\mathbf{p}}{(2\pi)^d} S_3(k,p,q) \frac{C^+(q)}{\beta_{(n)}(p)p^2}, \quad (63)$$

$$\begin{aligned} \delta\psi_{(n)}(k) &= \frac{1}{(d-1)k^2} \int^{\Delta} \frac{d\mathbf{p}}{(2\pi)^d} C^+(q) \left[S_3(k,p,q) \frac{1}{\beta_{(n)}(q)q^2} + S_2(k,p,q) \frac{\alpha_{(n)}(q)}{\beta_{(n)}(q)} \left(\frac{1}{\beta_{(n)}(p)p^2 + \beta_{(n)}(q)q^2} - \frac{1}{\beta_{(n)}(p)p^2} \right) \right. \\ &\left. + S_4(k,p,q) \frac{\alpha_{(n)}(p)}{\beta_{(n)}(p)} \frac{1}{\beta_{(n)}(q)q^2} \right], \end{aligned} \quad (64)$$

$$\delta\beta_{(n)}(k) = \frac{1}{(d-1)k^2} \int^{\Delta} \frac{d\mathbf{p}}{(2\pi)^d} S_1(k, p, q) \frac{C^+(q)}{\beta_{(n)}(p)p^2}. \quad (65)$$

Note that $\delta\alpha$, $\delta\beta$, $\delta\zeta$, $\delta\psi$, and hence α , β , ζ , ψ , are all independent of r . To solve the above equations, we substitute the following one-dimensional energy spectra in the above equations:

$$E^+(k) = K^+ \frac{(\Pi^+)^{4/3}}{(\Pi^-)^{2/3}} k^{-5/3}, \quad (66)$$

$$E^-(k) = rE^+(k). \quad (67)$$

For the elements of $\hat{\nu}$ we substitute

$$Z_{(n)}(k) = Z_{(n)}^* \sqrt{K^+} \frac{(\Pi^+)^{2/3}}{(\Pi^-)^{1/3}} k^{-4/3}, \quad (68)$$

where Z stands for ζ , α , ψ , β . The renormalized Z^* 's are calculated using the procedure outlined in the previous section. For large n their values for $d=3$ are

$$\hat{Z}^* = \begin{pmatrix} 0.86r & 0.14 \\ 0.16r & 0.84 \end{pmatrix}, \quad (69)$$

and for $d=2$ they are

$$\hat{Z}^* = \begin{pmatrix} 0.95r & 0.54 \\ 1.10r & 0.54 \end{pmatrix}. \quad (70)$$

Note that the solution converges for both $d=2$ and $d=3$.

As discussed in the earlier section, the cascade rates Π^{\pm} can be calculated from the renormalized parameters discussed above. Using the energy equations we can easily derive the equations for the cascade rates, which are

$$\Pi^+ = \int_0^{k_N} 2r\zeta k^2 E^+(k) + \int_0^{k_N} 2\alpha k^2 [E^u(k) - E^b(k)], \quad (71)$$

$$\Pi^- = \int_0^{k_N} 2\beta k^2 E^-(k) + \int_0^{k_N} 2r\psi k^2 [E^u(k) - E^b(k)]. \quad (72)$$

Under the assumption that $r_A=1$, the parts of Π^{\pm} proportional to $[E^u(k) - E^b(k)]$ vanish. Hence, the total cascade rate will be

$$\Pi = \frac{1}{2} (\Pi^+ + \Pi^-) \quad (73)$$

$$= r \int_0^{k_N} (\zeta + \beta) k^2 E^+(k). \quad (74)$$

Since ζ and β are independent of r , the total cascade rate is proportional to r (for r small). Clearly the cascade rate Π vanishes when $r=0$ or $\sigma_c=1$. This result is consistent with the fact that the nonlinear interactions are absent when only pure Alfvén waves (z^+ or z^-) are present. The detailed calculation of the cascade rates Π^{\pm} and the constants K^{\pm} is left for future studies (paper II).

IV. SUMMARY AND CONCLUSIONS

In this paper we have constructed a self-consistent RG scheme for MHD turbulence and computed the renormalized viscosity and resistivity. These quantities find applications in simulations specially large-eddy simulations (LES). In our RG scheme we assume that we are in the fully nonlinear range, and the renormalized energy spectrum is substituted for the correlation function. After the substitution of the correlation function, the renormalized Green's function or renormalized viscosity and resistivity are computed iteratively. In our procedure Kolmogorov's power law is taken for the energy spectrum, and it is shown to be a self-consistent solution of the RG equation for $d \geq d_c \approx 2.2$. This result is consistent with the recent theoretical,^{10,21,22} numerical,¹⁸⁻²⁰ and observational studies of solar wind^{16,17} that favor Kolmogorov's spectrum for MHD turbulence. Note that we do not carry out vertex (the coefficient of the nonlinear term) renormalization; there is an implicit assumption that the vertex renormalization, if any, is included when we substitute renormalized energy spectrum (Kolmogorov's) in the RG equation.

For simplicity of the calculation we have taken two special cases: (1) $\sigma_c=0$ and a full range of r_A ; (2) $\sigma_c \rightarrow 1$ and $r_A=1$. For these two cases, the renormalized viscosity and resistivity have been calculated for various space dimensions. For $\sigma_c=0$, there exists a stable RG fixed point for $d_1 \geq d_c \approx 2.2$. The RG fixed point is unstable for $d < d_c$. Our result is consistent with that Liang and Diamond,⁹ where they conclude that the RG fixed point for $d=2$ is unstable. Note, however, that the stability depends on the value of r_A and σ_c . An exhaustive study is required to ascertain the boundary of stability as a function of d , σ_c , and r_A .

Some interesting trends emerge as we vary space dimensionality. For $r_A=1$, the parameters ν^{ub*} and η^{bb*} decrease with the increase of d , but ν^{uu*} and η^{bu*} first increase until $d \approx 5$ then decrease.

For $d=3$, the variation of r_A shows some interesting features. For large r_A , ν^* is close to the ν^* for pure fluid turbulence, but η^* is also finite for this case. As r_A is decreased, ν^* increases and η^* decreases, or $\text{Pr} = \nu/\eta$ increases. Another important result of our calculation is the absence of turbulence for all r_A below 0.25 or so. In the $r_A \rightarrow 0$ (fully magnetic) limit, the MHD equations become linear; hence there is no turbulence. It is, however, surprising that turbulence disappears near $r_A=0.25$ itself.

Our RG calculation for fluid turbulence ($r_A=\infty$) show several interesting features. The RG fixed point is stable for $d=2$, and the renormalized viscosity is approximately -0.5 , a *negative* number. This is consistent with the inverse cascade of energy for the $\frac{5}{3}$ region. Note, however, that for $d=3$, the renormalized fluid viscosity is positive (0.38), hence the energy cascade is forward, consistent with Kolmogorov's hypothesis.

The values of the renormalized viscosity and resistivity calculated by our calculation differs from that of Verma and Bhattacharjee,³⁰ the later calculation being similar to Kraichnan's direct-interaction-approximation calculation for fluid turbulence. Verma and Bhattacharjee³⁰ assumed $\nu^{++} = \nu^{--}$

and $\nu^{+-} = \nu^{--}$, which is correct only in a limited region of parameter space. In addition, they assumed a cutoff for the self-energy calculation to cure infrared divergence. In the present calculation we have overcome both these defects, and expect that the numbers reported here will match with the future simulation results. It is unfortunate that the RG scheme fails for $d=2$; hence, several numerical results of 2D-MHD turbulence^{18–20,29} could not be compared with the analytic results presented here.

Kraichnan’s $\frac{3}{2}$ energy spectrum and $\Sigma^{uu} = \Sigma^{bb} \propto (kB_0)$ do not satisfy renormalization group equations [Eqs. (33)–(36)]. Hence $E(k) \propto k^{-3/2}$ is not a consistent solution of RG equations. This result is in agreement with the recent calculation by Verma,¹⁰ where it was shown that $B_0 = \text{const}$ does not satisfy RG equations, but the renormalized mean magnetic field ($B_0 \propto k^{-1/3}$) and Kolmogorov’s energy spectrum ($k^{-5/3}$) do satisfy the RG equations. From these arguments we can claim that Kraichnan’s $\frac{3}{2}$ power law is ruled out for strong MHD turbulence. However, $k^{-3/2}$ may still be considered in the framework of weak turbulence theory.

In our calculation we take $r_A(k) = E^u(k)/E^b(k)$ to be a constant. The global Alfvén ratio E^u/E^b may differ significantly from $r_A(k)$, still we make the approximation $r_A(k) = r_A$ to simplify the calculation. Similarly, we have assumed that $\sigma_c(k) = \text{const} = \sigma_c$. In addition, we also assume isotropy, which does not hold in the large r_A limit. It is hoped that future calculations will be able to relax these assumptions and attempt solutions for more realistic situations.

In many of the earlier RG calculations,^{1,4} it is assumed that the dynamical system under consideration is forced by

random noise at all scales. In those calculations, the noise and the vertex (coefficient of the nonlinear term) usually get renormalized along with the renormalization of dissipative coefficients. In contrast, in our scheme only the dissipative constants are renormalized, and the renormalization correction to other parameters (e.g., noise) are implicitly lumped into the full correlation function by assuming Kolmogorov’s power law. Our procedure is relatively simple, and one can easily calculate various interesting quantities. We hope that future developments in dynamical RG will be able to justify some of the assumptions made in our procedure.

To conclude, we have applied the RG procedure to MHD turbulence and calculated the renormalized viscosity and resistivity. These parameters find applications in simulations. We have shown that that Kolmogorov’s spectrum is a consistent solution of a MHD RG equation. The results presented here are in general agreement with the recent EDQNM and numerical results. Validation of the results presented here with numerical simulations will give us important insights into the physics of MHD turbulence.

ACKNOWLEDGMENTS

The author thanks J. K. Bhattacharjee for valuable discussions and insights from the inception to the end of the problem. The author also benefitted greatly from the numerous discussions he had with G. Dar and V. Eswaran on simulation results.

APPENDIX A: PERTURBATIVE CALCULATION OF MHD EQUATIONS

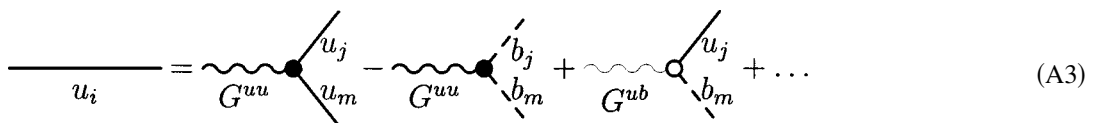
The MHD equations (7), (8) can be written as

$$\begin{pmatrix} u_i(\hat{k}) \\ b_i(\hat{k}) \end{pmatrix} = \begin{pmatrix} G^{uu}(\hat{k}) & G^{ub}(\hat{k}) \\ G^{bu}(\hat{k}) & G^{bb}(\hat{k}) \end{pmatrix} \begin{pmatrix} -\frac{i}{2} P_{ijm}^+(\mathbf{k}) \int d\hat{p} [u_j(\hat{p})u_m(\hat{k}-\hat{p}) - b_j(\hat{p})b_m(\hat{k}-\hat{p})] \\ -i P_{ijm}^-(\mathbf{k}) \int d\hat{p} [u_j(\hat{p})b_m(\hat{k}-\hat{p})] \end{pmatrix}, \tag{A1}$$

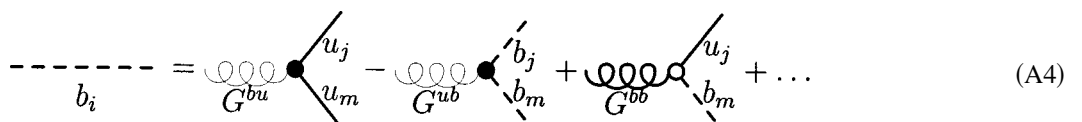
where the Green’s function G can be obtained from $G^{-1}(\hat{k})$,

$$G^{-1}(k, \omega) = \begin{pmatrix} -i\omega - \Sigma^{uu} & \Sigma^{ub} \\ \Sigma^{bu} & -i\omega - \Sigma^{bb} \end{pmatrix}. \tag{A2}$$

We solve the above equation perturbatively keeping the terms to the first order (nonvanishing). As usual, we represent the integrals by Feynmann diagrams. To leading order, the quantities u_i and b_i are expanded as



The diagram shows the expansion of the variable u_i (represented by a solid line) into a series of terms. The first term is a vertex labeled G^{uu} with two external lines labeled u_j and u_m . The second term is a vertex labeled G^{uu} with two external lines labeled b_j and b_m . The third term is a vertex labeled G^{ub} with two external lines labeled u_j and b_m . The expansion is followed by an ellipsis $+\dots$. The equation is labeled (A3).



The diagram shows the expansion of the variable b_i (represented by a dashed line) into a series of terms. The first term is a vertex labeled G^{bu} with two external lines labeled u_j and u_m . The second term is a vertex labeled G^{ub} with two external lines labeled b_j and b_m . The third term is a vertex labeled G^{bb} with two external lines labeled u_j and b_m . The expansion is followed by an ellipsis $+\dots$. The equation is labeled (A4).

The variables u and b are represented by solid and dashed lines, respectively. The quantity G^{uu} , G^{ub} , G^{bb} , G^{bu} are represented by thick wiggly (photon), thin wiggly, thick curly (gluon), and thin curly lines, respectively. The filled circle represents a $(-i/2)P_{ijm}^+$ vertex, while the empty circle represents a $-iP_{ijm}^-$ vertex.

The substitution of $u_i^>$ and $b_i^>$ in the second bracketed terms of Eqs. (16), (17), denoted by I_2^u and I_2^b , respectively, will yield

$$I_2^u = \begin{array}{c} \diagup \\ \bullet \\ \diagdown \end{array} \begin{array}{c} \diagup \\ \diagdown \\ \diagdown \end{array} - \begin{array}{c} \diagup \\ \bullet \\ \diagdown \end{array} \begin{array}{c} \diagup \\ \diagdown \\ \diagdown \end{array} \quad (A5)$$

$$I_2^b = \begin{array}{c} \diagup \\ \circ \\ \diagdown \end{array} \begin{array}{c} \diagup \\ \diagdown \\ \diagdown \end{array} + \begin{array}{c} \diagup \\ \circ \\ \diagdown \end{array} \begin{array}{c} \diagup \\ \diagdown \\ \diagdown \end{array} \quad (A6)$$

We illustrate the expansion of one of the above diagrams:

$$\begin{array}{c} \begin{array}{c} \diagup \\ \bullet \\ \diagdown \end{array} \begin{array}{c} \diagup \\ \diagdown \\ \diagdown \end{array} = 2 \begin{array}{c} \text{wavy} \\ \bullet \\ \text{wavy} \end{array} \begin{array}{c} \text{wavy} \\ \text{wavy} \\ \text{wavy} \end{array} + \begin{array}{c} \text{wavy} \\ \bullet \\ \text{wavy} \end{array} \begin{array}{c} \text{wavy} \\ \text{wavy} \\ \text{dashed} \end{array} + \begin{array}{c} \text{wavy} \\ \bullet \\ \text{wavy} \end{array} \begin{array}{c} \text{wavy} \\ \text{dashed} \\ \text{dashed} \end{array} + 2 \begin{array}{c} \text{wavy} \\ \bullet \\ \text{wavy} \end{array} \begin{array}{c} \text{wavy} \\ \text{dashed} \\ \text{dashed} \end{array} - \\ 2 \begin{array}{c} \text{dotted} \\ \bullet \\ \text{dotted} \end{array} \begin{array}{c} \text{wavy} \\ \text{wavy} \\ \text{wavy} \end{array} - \begin{array}{c} \text{dotted} \\ \bullet \\ \text{dotted} \end{array} \begin{array}{c} \text{wavy} \\ \text{wavy} \\ \text{dashed} \end{array} - \begin{array}{c} \text{dotted} \\ \bullet \\ \text{dotted} \end{array} \begin{array}{c} \text{wavy} \\ \text{dashed} \\ \text{dashed} \end{array} - 2 \begin{array}{c} \text{dotted} \\ \bullet \\ \text{dotted} \end{array} \begin{array}{c} \text{wavy} \\ \text{dashed} \\ \text{dashed} \end{array} + \\ \begin{array}{c} \text{wavy} \\ \circ \\ \text{wavy} \end{array} \begin{array}{c} \text{wavy} \\ \text{wavy} \\ \text{wavy} \end{array} + \begin{array}{c} \text{wavy} \\ \circ \\ \text{wavy} \end{array} \begin{array}{c} \text{wavy} \\ \text{wavy} \\ \text{dashed} \end{array} + \begin{array}{c} \text{wavy} \\ \circ \\ \text{wavy} \end{array} \begin{array}{c} \text{wavy} \\ \text{dashed} \\ \text{dashed} \end{array} + \begin{array}{c} \text{wavy} \\ \circ \\ \text{wavy} \end{array} \begin{array}{c} \text{wavy} \\ \text{dashed} \\ \text{dashed} \end{array} + \\ \begin{array}{c} \text{dotted} \\ \circ \\ \text{dotted} \end{array} \begin{array}{c} \text{wavy} \\ \text{wavy} \\ \text{wavy} \end{array} + \begin{array}{c} \text{dotted} \\ \circ \\ \text{dotted} \end{array} \begin{array}{c} \text{wavy} \\ \text{wavy} \\ \text{dashed} \end{array} + \begin{array}{c} \text{dotted} \\ \circ \\ \text{dotted} \end{array} \begin{array}{c} \text{wavy} \\ \text{dashed} \\ \text{dashed} \end{array} + \begin{array}{c} \text{dotted} \\ \circ \\ \text{dotted} \end{array} \begin{array}{c} \text{wavy} \\ \text{dashed} \\ \text{dashed} \end{array} \end{array} \quad (A7)$$

In the above diagrams solid lines denote C^{uu} , and the dotted lines denote C^{ub} . The correlation function C^{bb} is denoted by a dashed line. As mentioned earlier, the wiggly and curly lines denote various Green's functions. All the diagrams except the fourth, eighth, twelfth, and sixteenth can be shown to be trivially zero using Eqs. (18)–(24). We assume that the fourth, eighth, twelfth, and sixteenth diagrams are also zero, as usually done in turbulence RG calculations.^{4,5} Similarly, we can show that all other diagrams of I_2^u and I_2^b are zero; hence, $I_2^u = I_2^b = 0$ to first order.

The third bracketed terms of (16), (17), denoted by I_3^u and I_3^b , respectively, are diagrammatically represented as

$$I_3^u = \begin{array}{c} \diagup \\ \bullet \\ \diagdown \end{array} \begin{array}{c} \diagup \\ \diagdown \\ \diagdown \end{array} - \begin{array}{c} \diagup \\ \bullet \\ \diagdown \end{array} \begin{array}{c} \diagup \\ \diagdown \\ \diagdown \end{array} \\ = -\delta\Sigma^{uu}(k) \begin{array}{c} \diagup \\ \diagdown \\ \diagdown \end{array} - \delta\Sigma^{ub}(k) \begin{array}{c} \diagup \\ \diagdown \\ \diagdown \end{array} \quad (A8)$$

$$I_3^b = \begin{array}{c} \diagup \\ \circ \\ \diagdown \end{array} \begin{array}{c} \diagup \\ \diagdown \\ \diagdown \end{array} \\ = -\delta\Sigma^{bu}(k) \begin{array}{c} \diagup \\ \diagdown \\ \diagdown \end{array} - \delta\Sigma^{bb}(k) \begin{array}{c} \diagup \\ \diagdown \\ \diagdown \end{array} \quad (A9)$$

where

$$-(d-1)\delta\Sigma^{uu} = 4 \text{ (diagram)} - 2 \text{ (diagram)} + 2 \text{ (diagram)} - 4 \text{ (diagram)} \quad (\text{A10})$$

$$-(d-1)\delta\Sigma^{ub} = -4 \text{ (diagram)} + 2 \text{ (diagram)} + 4 \text{ (diagram)} - 2 \text{ (diagram)} \quad (\text{A11})$$

$$-(d-1)\delta\Sigma^{bu} = 2 \text{ (diagram)} + \text{ (diagram)} + \text{ (diagram)} - 2 \text{ (diagram)} \quad (\text{A12})$$

$$-(d-1)\delta\Sigma^{bb} = 2 \text{ (diagram)} + \text{ (diagram)} + \text{ (diagram)} - \text{ (diagram)} \quad (\text{A13})$$

In Eqs. (A10)–(A13) we have omitted all the vanishing diagrams (similar to those appearing in I_2). Looking at all the terms, we observe that I_3^u contributes to Σ^{uu} and Σ^{ub} renormalization, while I_3^b contributes to Σ^{bb} and Σ^{bu} renormalization. The algebraic expressions for the above diagrams are given by Eqs. (27)–(30).

APPENDIX B: VALUES OF S_i

Here $S_i(k, p, q)$ are formed by contracting tensors P_{ijm}^+ , P_{ijm}^- , P_{ij} , and M_{ijm} [see Eqs. (11), (13), and (50)]. On simplification, S_i 's become functions of k, p, q , and cosines x, y, z , defined as

$$\mathbf{p} \cdot \mathbf{q} = -pqx; \quad \mathbf{q} \cdot \mathbf{k} = qky; \quad \mathbf{p} \cdot \mathbf{k} = pkz. \quad (\text{B1})$$

The algebraic expressions for various $S_i(k, p, q)$ are given below:

$$S_1(k, p, q) = M_{bjm}(k)M_{mab}(p)P_{ja}(q) = kp(d-2+z^2)(z+xy), \quad (\text{B2})$$

$$S_2(k, p, q) = M_{ajm}(k)M_{mab}(p)P_{jb}(q) = kp(-z+z^3+y^2z+xyz^2), \quad (\text{B3})$$

$$S_3(k, p, q) = M_{bjm}(k)M_{jab}(p)P_{ma}(q) = kp(-z+z^3+x^2z+xyz^2), \quad (\text{B4})$$

$$S_4(k, p, q) = M_{ajm}(k)M_{jab}(p)P_{mb}(q) = kp(-z+z^3+xy+x^2z+y^2x+xyz^2), \quad (\text{B5})$$

$$S(k, p, q) = P_{bjm}^+(k)P_{mab}^+(p)P_{ja}(q) = kp[(d-3)z+2z^3+(d-1)xy], \quad (\text{B6})$$

$$S_5(k, p, q) = P_{bjm}^+(k)P_{mab}^-(p)P_{ja}(q) = kp[(d-1)z+(d-3)xy-2y^2z], \quad (\text{B7})$$

$$S_6(k, p, q) = P_{ajm}^+(k)P_{mba}^-(p)P_{jb}(q) = -S_5(k, p, q), \quad (\text{B8})$$

$$S_7(k, p, q) = P_{ijm}^-(k)P_{mab}^+(p)P_{ja}(q)P_{ib}(k) = S_5(p, k, q), \quad (\text{B9})$$

$$S_8(k, p, q) = P_{ijm}^-(k)P_{jab}^+(p)P_{ma}(q)P_{ib}(k) = -S_5(p, k, q), \quad (\text{B10})$$

$$S_9(k, p, q) = P_{ijm}^-(k)P_{mab}^-(p)P_{ja}(q)P_{ib}(k) = kp(d-1)(z+xy), \quad (\text{B11})$$

$$S_{10}(k, p, q) = P_{ijm}^-(k)P_{mab}^-(p)P_{jb}(q)P_{ia}(k) = -S_9(k, p, q), \quad (\text{B12})$$

$$S_{11}(k, p, q) = P_{ijm}^-(k)P_{jab}^-(p)P_{ma}(q)P_{ib}(k) = -S_9(k, p, q), \quad (\text{B13})$$

$$S_{12}(k, p, q) = P_{ijm}^-(k)P_{jab}^-(p)P_{mb}(q)P_{ia}(k) = S_9(k, p, q). \quad (\text{B14})$$

There are many useful relationships between $S_i(k, p, q)$'s. Some of them are

$$S(k, p, q) = S_1(k, p, q) + S_2(k, p, q) + S_3(k, p, q) + S_4(k, p, q), \quad (\text{B15})$$

$$S_5(k, p, q) = S_1(k, p, q) - S_2(k, p, q) + S_3(k, p, q) - S_4(k, p, q). \quad (\text{B16})$$

- ¹D. Forster, D. R. Nelson, and M. J. Stephen, *Phys. Rev. A* **16**, 732 (1977).
- ²C. DeDominicis and P. C. Martin, *Phys. Rev. A* **19**, 419 (1979).
- ³J. D. Fournier and U. Frisch, *Phys. Rev. A* **17**, 747 (1978).
- ⁴V. Yakhot and S. A. Orszag, *J. Sci. Comput.* **1**, 3 (1986).
- ⁵W. D. McComb, *The Physics of Fluid Turbulence* (Clarendon, Oxford, 1990).
- ⁶W. D. McComb, *Rep. Prog. Phys.* **58**, 1117 (1995).
- ⁷J. D. Fournier, P.-L. Sulem, and A. Pouquet, *J. Phys. A* **15**, 1393 (1982).
- ⁸S. J. Camargo and H. Tasso, *Phys. Fluids B* **4**, 1199 (1992).
- ⁹W. Z. Liang and P. H. Diamond, *Phys. Fluids B* **5**, 63 (1993).
- ¹⁰M. K. Verma, *Phys. Plasmas* **6**, 1455 (1999).
- ¹¹R. H. Kraichnan, *Phys. Fluids* **8**, 1385 (1965).
- ¹²P. S. Iroshnikov, *Sov. Astron.* **7**, 566 (1964).
- ¹³W. H. Matthaeus and Y. Zhou, *Phys. Fluids B* **1**, 1929 (1989).
- ¹⁴Y. Zhou and W. H. Matthaeus, *J. Geophys. Res.* **95**, 10 291 (1990).
- ¹⁵E. Marsch, in *Reviews in Modern Astronomy*, edited by G. Klare (Springer-Verlag, Berlin, 1990), p. 43.
- ¹⁶W. H. Matthaeus and M. L. Goldstein, *J. Geophys. Res.* **87**, 6011 (1982).
- ¹⁷E. Marsch and C.-Y. Tu, *J. Geophys. Res.* **95**, 8211 (1990).
- ¹⁸M. K. Verma, D. A. Roberts, M. L. Goldstein *et al.*, *J. Geophys. Res.* **101**, 21 619 (1996).
- ¹⁹W. C. Müller and D. Biskamp, *Phys. Rev. Lett.* **84**, 475 (2000).
- ²⁰D. Biskamp and W. C. Müller, *Phys. Plasmas* **7**, 4889 (2000).
- ²¹S. Sridhar and P. Goldreich, *Astrophys. J.* **432**, 612 (1994).
- ²²P. Goldreich and S. Sridhar, *Astrophys. J.* **438**, 763 (1995).
- ²³Y. Zhou and G. Vahala, *Phys. Rev. E* **47**, 2503 (1993).
- ²⁴J. D. Fournier, U. Frisch, and A. Rose, *J. Phys. A* **11**, 187 (1978).
- ²⁵W. D. McComb and A. G. Watt, *Phys. Rev. A* **46**, 4797 (1992).
- ²⁶A. Pouquet, *J. Fluid Mech.* **88**, 1 (1994).
- ²⁷A. Ishizawa and Y. Hattori, *J. Phys. Soc. Jpn.* **67**, 4302 (1998).
- ²⁸A. Ishizawa and Y. Hattori, *J. Phys. Soc. Jpn.* **67**, 441 (1998).
- ²⁹G. Dar, M. K. Verma, and V. Eswaran, *Physica D* (to be published).
- ³⁰M. K. Verma and J. K. Bhattacharjee, *Europhys. Lett.* **31**, 195 (1995).